Using ^{14}C-Dated Peat Beds for Reconstructing Subsidence by Compression in the Holland Coastal Plain of the Netherlands

Author(s): Kay Koster, Kim M. Cohen, Jan Stafleu, and Esther Stouthamer

Source: Journal of Coastal Research, 34(5):1035-1045.
Published By: Coastal Education and Research Foundation
https://doi.org/10.2112/JCOASTRES-D-17-00093.1
URL: http://www.bioone.org/doi/full/10.2112/JCOASTRES-D-17-00093.1

Journal of Coastal Research	34	5	1035–1045	Coconut Creek, Florida	September 2018

Using ^{14}C-Dated Peat Beds for Reconstructing Subsidence by Compression in the Holland Coastal Plain of the Netherlands

Kay Koster[†‡*], Kim M. Cohen[†‡§], Jan Stafleu[‡], and Esther Stouthamer[†]

[†]Department of Physical Geography
Faculty of Geosciences, Utrecht University
Utrecht, The Netherlands

[‡]Department of Geomodeling
TNO Geological Survey of the Netherlands
Utrecht, The Netherlands

[§]Department of Applied Geology and Geophysics
Deltares
Utrecht, The Netherlands

www.cerf-jcr.org

www.JCRonline.org

ABSTRACT

Koster, K.; Cohen, K.M.; Stafleu, J., and Stouthamer, E., 2018. Using ^{14}C-dated peat beds for reconstructing subsidence by compression in the Holland coastal plain of the Netherlands. *Journal of Coastal Research,* 34(5), 1035–1045. Coconut Creek (Florida), ISSN 0749-0208.

Subsidence in the Holland coastal plain of the Netherlands was reconstructed from the vertical displacement of Holocene peat layers below their reference groundwater levels at the time of peat formation. This quantifies the part of subsidence that is due to compression processes and allows specification of the current state of peat compression in a map. ^{14}C-dating of peat layers found intercalated in the Holocene sequence were used in the reconstruction. This dataset was combined with results from a recent coastal-deltaic plain wide three-dimensional (3D) interpolation of reference palaeo-groundwater levels, at which the intercalated peats are thought to have formed before they were buried, compressed, and vertically displaced. Empiric relations between reconstructed displacement and the thickness of overburden were determined and deployed in a national 3D geological subsurface model to establish a subsidence map with continuous cover of the coastal plain. The resulting maps show compressed peat layers under urbanized areas with 1 to 8 m of natural and anthropogenic overburden have subsided 1 to 5 m below the original level of formation. In the agricultural area of the coastal plain, where overburden is merely decimetres thick, consisting of fluvial flood- and sea-ingression deposits, peat generally experienced less than 1 m subsidence. The reference-level reconstruction method is deployable over large coastal plain areas to reconstruct subsidence caused by postdepositional vertical displacement of intercalated peat layers. It could therefore serve as an alternative approach for methods based on soil mechanics, which require input often not available for coastal plains on regional scales.

ADDITIONAL INDEX WORDS: *Peat compression, Holocene, coastal subsidence.*

INTRODUCTION

Many populated Holocene coastal plains and deltas are subsiding, resulting in increased flood risks, saltwater intrusion, and damaged infrastructures (Higgins, 2016; Syvitski *et al.*, 2009). In the case of peat-rich coastal-deltaic plains, this is predominantly caused by the process of compression and oxidation that both affect shallow subsurface Holocene peat layers (Gambolati *et al.*, 2006) (Figure 1). Compression is the densification of peat induced by increasing vertical effective stress (Den Haan, 1994). This results from groundwater level lowering (now notably in agricultural areas), from overburden (now notably in urban regions), and from time-dependent creep processes that occur regardless of changes in vertical effective stress (Den Haan, 1994). Peat oxidation comprises the decomposition of organic matter by aeration and prevails during periods of low groundwater levels (Hooijer *et al.*, 2012; Wösten, Ismail, and Van Wijk, 1997). Compression of clayey coastal-deltaic deposits causes additional subsidence, albeit modestly compared with the peat contributions (Koster, Erkens, and Zwanenburg, 2016). Consequently, compression causes Holocene peat layers to be found vertically displaced below their initial level of formation. Studies from the peat-rich Mississippi delta (Törnqvist *et al.*, 2008), Sacramento–San Joaquin delta (Drexler, De Fontain, and Deverel, 2009), Rhine–Meuse delta (Van Asselen, 2011), Fraser delta (Mazzotti *et al.*, 2009), and the Venice lagoon (Gambolati *et al.*, 2006) exemplify this form of land subsidence.

In the peat-rich Holocene coastal plain of the Netherlands (*ca.* 17,000 km^2), large areas (*ca.* 50%) are situated below sea level due to subsidence by peat compression and oxidation (Figure 2A). The subsidence is to a large extent human induced and commenced around AD 1000, when coastal wetlands were extensively drained for agricultural purposes (Borger, 1992). As a consequence, considerable areas of reclaimed peatlands were flooded by sea ingressions during the past 1000 years (Pierik *et al.*, 2017; Vos, 2015). Additional overburden was deposited on the coastal wetland peat by the ingressions, inducing further compression and vertical lowering of the peat. Inhabitants reacted to these floods by artificially raising the land surface with sediments and household waste (Koster, 2016), thereby locally compressing and vertically displacing the peat even more (Kluiving *et al.*, 2016). Peat mining independently has caused surface lowering, mainly in areas that

DOI: 10.2112/JCOASTRES-D-17-00093.1 received 15 May 2017; accepted in revision 18 December 2017; corrected proofs received 20 February 2018; published pre-print online 26 March 2018.
*Corresponding author: kay.koster@tno.nl

Figure 1. Examples of peat-rich coastal-deltaic plains subjected to various degrees of anthropogenic use and associated subsidence. From left to right: Cumberland marshes, Canada; a pristine inland delta that does not experience human-induced subsidence. Mississippi delta, United States; a delta that is partly subsiding due to anthropogenic processes since the 20th century. Holland coastal plain, the Netherlands; a coastal plain under complete anthropogenic control that is experiencing severe subsidence for many centuries (photos courtesy of S. van Asselen, J. Wark, and Rijksdienst voor het Cultureel Erfgoed). (Color for this figure is available in the online version of this paper.)

escaped ingressions and river flooding (Borger, 1992). As a result of this history, the levels at which peat beds are now encountered hold a record of vertical displacement that show a heterogeneous pattern of superposed natural preconditions, reclamation styles, ingression cover, and artificially raised surfaces (Pierik *et al.*, 2017; Van Asselen, Stouthamer, and Van Asch, 2009).

Although peat-related subsidence has long been recognized in the Netherlands (Huizinga, 1940; Schothorst, 1977), the rates at which subsidence is proceeding, spatial variability herein, and its influence on modern land use have only recently been addressed (Stouthamer and Van Asselen, 2015; Van den Born *et al.*, 2016). Reconstructing and mapping past peat-related subsidence is an important step to assess and manage present day and future subsidence across the urbanized coastal plain. This provides causal insight between the spatial variations in peat occurrences and thickness of overburden. Furthermore, it is essential to create awareness among stakeholders and policy makers regarding the threat of land subsidence that at some point may stop being manageable using present land practices (Van den Born *et al.*, 2016).

This study explores at the coastal plain scale how reconstructions of vertical displacement of peat beds from large ^{14}C datasets is useful in subsidence research, with a focus on the compression-caused component. The aims of this study are twofold. First, the potential of a ^{14}C-dating based regression

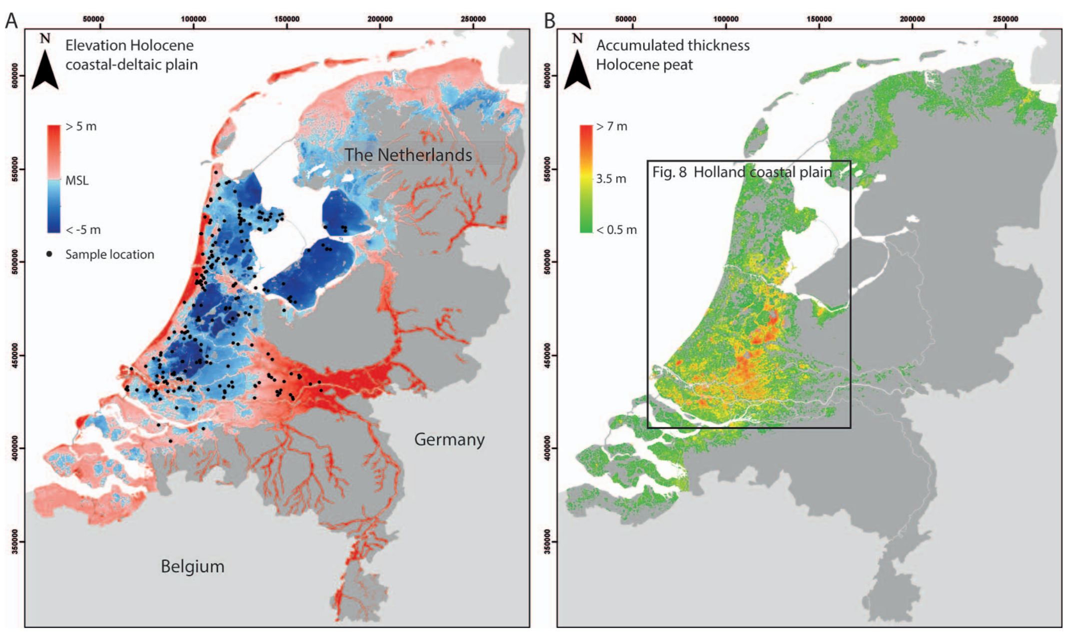

Figure 2. (A) Surface elevation of the Holocene coastal-deltaic plain in the Netherlands relative to mean sea level (MSL) and ^{14}C-dating sample locations. (B) Accumulated thickness of peat in the Holocene sequence of the coastal-deltaic plain extracted from the 3D geological subsurface model GeoTOP (TNO-GSN, 2016). The rectangle represents the final focus area of the subsidence map. (Color for this figure is available in the online version of this paper.)

method developed for quantifying peat compression on local scales was investigated, to reconstruct and quantify subsidence by peat compression on a regional scale. A large set of ^{14}C-dated intercalated peat layers was collected from the heavily urbanized coastal plain of Holland, the Netherlands (*ca.* 12,400 km^2) (Figure 2B). Second, a map of this area showing the amount of subsidence that Holocene peat experienced by compression was produced.

Previous Work

At the local scale of single sites, reconstructions of compression-induced subsidence have been developed and deployed in Holocene relative sea-level rise research (Brain, 2016; Brain *et al.*, 2012; Massey *et al.*, 2006), and similarly in studies relating natural overburden to compressibility of buried peat beds (Van Asselen, 2011). Methodologically, such studies determine at a high vertical resolution current physical properties of cored peat layers and use that as input for soil-mechanics models focusing on primary and secondary compression. Reconstructing subsidence on a large spatial scale using this approach, however, is not straightforward, since it requires input of physical peat properties, timing of compression, stress histories, and duration of successive compression stages. These are spatially variable and often unknown. Consequently, soil mechanics is at present impractical to apply on large spatial scales. Erkens, Van der Meulen, and Middelkoop (2016) exemplified these challenges, as they used a spatiotemporal constant for peat organic matter dry density to reconstruct compression coastal peat experienced in the Netherlands during the past 1000 years, because variations herein could not be determined.

Sea-level reconstruction uses ^{14}C-dated coastal peat beds as proxy data for former lagoon and estuarine sea levels, provided that their sample level can be converted to an original level. To do so for intercalated peat beds, the sea-level reconstruction community developed empirical approaches to quantify subsidence by compression of peat beds based on ^{14}C-dating (Bloom, 1964; Edwards, 2006; Horton *et al.*, 2013; Horton and Shennan, 2009; Long, Waller, and Stupples, 2006; Meckel, Ten Brink, and Williams, 2007; Roberts, Bailey, and Kuecher, 1994; Shennan *et al.*, 2000; Törnqvist *et al.*, 2008; Van Asselen, 2011).

One approach empirically explores regression-fit functions with coefficients calibrated on the vertical differences between (1) reconstructed relative water level position at the time of peat formation (^{14}C-dated age), and (2) the present elevation level of the peat (*z* position of ^{14}C-dated sample). This offset is equal to the amount of subsidence experienced by the peat bed that is due to the compression of the peat layer itself and that of underlying compressible deposits. The function fits typically describe the amount of subsidence as depending on (1) thickness of the younger overburden, which is responsible for the compression of the intercalated peat layer and underlying deposits, and (2) depth to the incompressible substrate, defining the vertical interval of the compressible Holocene deposits underlying the sampled peat layer. Edwards (2006) and Shennan *et al.* (2000) and provide linear regression relations between the compression-induced subsidence (termed by them 'sediment consolidation' or 'compaction') and 'thickness of overburden' and 'depth to substrate', and successfully applied them in Holocene sea-level reconstructions for the U.K. Such linear relations have also been found for other coastal-deltaic sequences that embed intercalated peat layers (Horton *et al.*, 2013; Horton and Shennan, 2009; Törnqvist *et al.*, 2008).

The challenge of the present study was to obtain regression-fit functions for a large heterogeneous dataset of ^{14}C-dated peat layers collected from an entire coastal plain. The Holland coastal plain case is suitable for this, because reference levels for this area have previously been reconstructed in three-dimensional (3D) interpolation (see below) (Cohen, 2005; Koster, Stafleu, and Cohen, 2016).

METHODS

Compression-induced subsidence of intercalated peat layers and underlying compressible substrate is reconstructed as the vertical difference between their initial and current position. To quantify past subsidence at a regional scale, the initial position (or reference level) and current level of ^{14}C-dated peat beds are required. Both should be of even coverage and quality across the coastal-deltaic plain. In this section, a rationale is provided elaborating on varying initial and current levels of peat layers in the study area. Next, the dataset is presented supplying the reference level across the study area by interpolation of a basal peat ^{14}C dataset (summarizing Koster, Stafleu, and Cohen, 2016). After that the dataset of vertically displaced peat beds is presented, *i.e.* ^{14}C-dates from intercalated peat layers. The section is completed by giving background information on a voxel-based 3D geological subsurface model of the study area, which was used as input regarding overburden and depth at the locations of the intercalated peat ^{14}C dataset and as the geomodelling framework for producing a subsidence map.

The schematic cross section of the Holland coastal plain (Figure 3) illustrates the various positions from where basal peat and intercalated peats have been sampled and their indication for water level positions at the time of peat formation and postdepositional displacements (compression) and removal (oxidation, mining). Furthermore, it shows the reference levels for coastal-deltaic peat formation of known age as stacked blue lines (reconstructed isochrons) that are known at each location where an intercalated peat bed still exists (*i.e.* has not oxidized or been mined) and has been radiocarbon dated. This delivers the vertical difference and quantifies the part of subsidence that is due to the compression of the peat layers itself and that of underlying Holocene deposits (*cf.* Shennan *et al.*, 2000).

The Holland coastal plain is experiencing differential subsidence of tectonic and glacial isostatic origin (Kiden, Denys, and Johnston, 2002; Kooi *et al.*, 1998). Consequently, intercalated peat layers subsided relative to a present day reference level, regardless of compression. In the reference levels, lateral elevation gradients were implemented to correct for subsidence by tectonics and isostasy (Cohen, 2005; Koster, Stafleu, and Cohen, 2016). Consequently, the vertical difference between the initial and present elevation of intercalated peat layers is solely caused by compression of the peat beds or the underlying Holocene deposits.

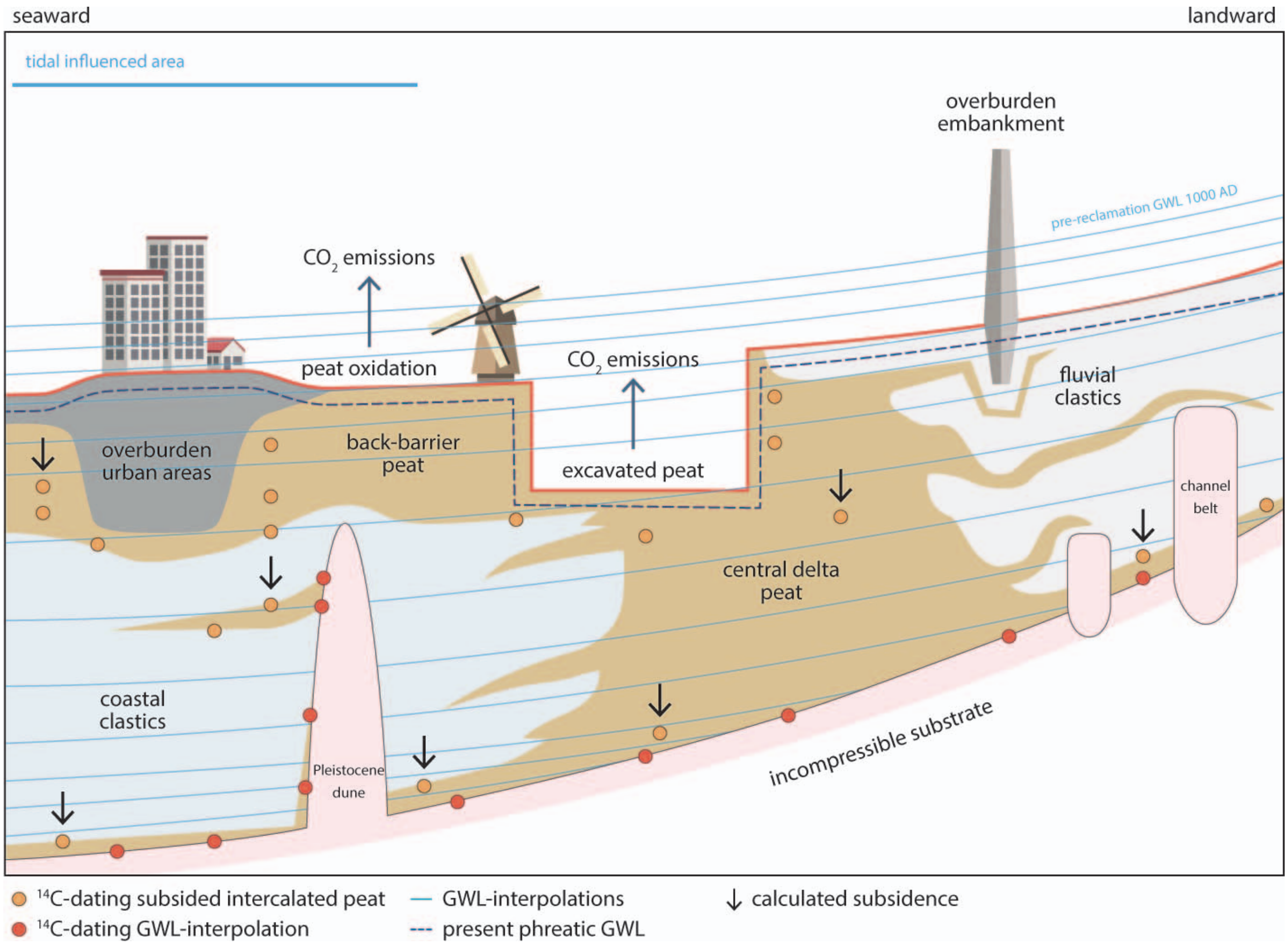

Figure 3. Schematic overview of the peat-rich coastal-deltaic sequence of the Netherlands subjected to differential subsidence as a result of peat compression, oxidation, and mining. Present day water levels are kept artificially below natural positions. Subsidence by peat compression is quantified by measuring the vertical distance between a reference level to which the peat initially formed and the depth where it was sampled. (Color for this figure is available in the online version of this paper.)

Reference Levels

A previously developed 3D interpolation of palaeo-groundwater levels (GWLs; Cohen, 2005; Koster, Stafleu, and Cohen, 2016) was used to determine the reference levels. The interpolation yields GWLs for the coastal plain of Holland for the period between 10,800 and 1000 calibrated years before present (cal BP) and is based on 384 ^{14}C-dating of basal peat (x, y, z, and age known). Basal peat originates from swamps in fluvial and coastal floodbasins that onlapped a seaward sloping Pleistocene surface (sloping between *ca*. 7 and –25 m relative to mean sea level). The 3D interpolation of the reference levels (z) was conducted on a grid in the x, y, age domain (resolution: 1000 × 1000 m × 200 y; with age in vertical direction). This interpolation method classifies as 3D block kriging with an external drift (Cohen, 2005), meaning that it was conducted in two steps. First, a regionalized trend function (*i.e.* the external drift) that describes spatiotemporal trends in Holocene groundwater level rise was fit (optimized for the basal peat ^{14}C data), and then a block-kriging interpolation procedure was carried out on the residuals to amend the trend function prediction of past water level elevations with subregional deviations (present in the data, but not captured with the trend function).

The input basal peat samples consist of *Alnus*, *Phragmites*, *Carex* peat, and undefined peat. These different peat types form in various ranges of water depths, and, consequently, their vertical position provides an indication of the elevation of the reference levels. Each peat type has a maximum water depth in which vegetation can develop (*cf*. Bos, Busschers, and Hoek, 2012; Den Held, Schmitz, and Van Wirdum, 1992): *Alnus* peat in fluvial floodbasins ±0.1 m, *Phragmites* peat in both fluvial and tidal floodbasins –1 m, and *Carex* peat in fluvial floodbasins –0.3 m. These maximum water depths were incorporated in the 3D interpolation as vertical uncertainties between the level of peat formation and coeval groundwater levels (σ_{peat}). They were attributed to each basal peat sample and incorporated in the statistical interpolation procedure as variances of measurement errors.

The interpolation includes a spatiotemporally quantified uncertainty (σ_{GWL}) that has a minimum of 0.13 m in data-rich areas and a maximum of 1.19 m in data-poor areas. During the interpolation the errors were processed as follows: $\sigma_{\text{vert.diff.}} = \sqrt{(\sigma^2_{\text{peat}} + \sigma^2_{\text{GWL}})}$, and the interpolation produced Holocene GWLs with vertical errors that range between *ca*. 0.4 m (*Alnus* peat data-rich areas), to *ca*. 2 m (undefined peat in data-poor areas).

A known deficiency of the GWL interpolation method is deficient because it lacks tidally raised regional levels that are otherwise known to have existed around tidal inlets (Koster, Stafleu, and Cohen, 2016). Peatlands fringing tidal inlets often form around groundwater levels at an elevation grading to mean high water, *i.e.* in the Netherlands close to a metre above contemporary mean sea level (Van der Spek, 1994; Vis *et al.*, 2015). Peat formation along the rims of larger lagoons and in wide fluvial-tidal floodbasins, however, occurs at a few decimetres lower, closer to contemporary sea level (Van de Plassche, 1995). The basal peat dataset used in the 3D interpolation contains index points from the latter setting only. Because the dimensions and morphology of tidal inlet systems have changed over time, the tidal amplitudes experienced in different inland sections of these systems have varied as well. Including a reconstruction of tidal ranges requires additional datasets and method development, which are not within the scope of this study. The GWL reference levels thus underestimate regional GWLs in certain seaward parts of the coastal plain around active funnelling tidal inlets (Koster, Stafleu, and Cohen, 2016).

Vertically Displaced Intercalated Peat Layers

Five hundred thirteen (513) ^{14}C-dating samples of intercalated peat layers was deployed for the subsidence regression analysis (see Figure 2A for the sample's spatial distribution and Supplementary Material for the dataset). The samples were taken from cored boreholes, and their elevation determined during sampling was regarded as the current vertical position. The samples were calibrated to calendar years BP (software, OxCal 4.2, Bronk Ramsey, 2009; reference curve, IntCal13, Reimer *et al.*, 2013). The GWL interpolation was used to look up the initial level of intercalated peat formation. This yielded a reconstructed initial elevation and associated error ($\sigma_{\text{vert.diff.}}$) per intercalated peat sample. Subsidence by compression was subsequently quantified as the difference between the initial and current position of the intercalated peat layers.

Regression Analysis and Subsidence Mapping

To assess the dependency of peat layer subsidence to overburden thickness and depth to substrate, linear regression analysis was used. Hereto, overburden thickness and depth to substrate were determined from the GeoTOP 3D geological subsurface voxel model (Stafleu *et al.*, 2011; Geological Survey of The Netherlands (TNO-GSN)). GeoTOP has a resolution of $100 \times 100 \times 0.5$ m, and each voxel is attributed with lithostratigraphic unit and lithology. It was used to specify the thickness of overburden and depth to substrate of each ^{14}C-dated intercalated peat layer. The thickness of overburden in the study area varies from less than 1 m for surficial peat layers to over 22 m for the top of basal peat layers. Depth to substrate ranged from several centimetres for the top of basal peat layers to over 20 m for coast-nearby surficial peat layers.

Voxels assigned as Holocene peat were extracted from GeoTOP to serve as input cells for the subsidence mapping. For the mapping, the vertical position of these cells relative to their position within the Holocene sequence was used as input for the obtained regression functions. This yielded compression-induced subsidence values, which were attributed to the selected Holocene peat cells.

Vertical effective stress (σ') is put forward here as an alternative for using overburden thickness in the regression analysis. It is widely acknowledged that the amount of primary compression a peat layer experienced is related to the vertical effective stress exerted by its overburden (Den Haan, 1994; Mesri and Ajlouni, 2007). During the dynamic build-up history of coastal-deltaic areas, groundwater levels and thickness of overburden, as well as the composition of overburden, continuously changes. Consequently, vertical effective stress exerted on intercalated Holocene peat beds changed as well. This complex interplay of stress changes influenced primary compression rates, the offset between reversible and irreversible compression, and creep rates. Therefore, the use of present day vertical effective stress can be regarded as a step forward to implement more variation in overburden in addition to its thickness. For more detailed analysis on the influence of vertical effective stress on past compression, maps indicating past physical peat properties and changes in stress regimes are necessary, but they are currently nonexistent.

Present day vertical effective stress exerted on each sampled intercalated peat layer was calculated as the difference between total stress (σ) and hydrostatic pressure (μ) prevailing at the sampling depth: $\sigma' = \sigma - \mu$. Kruiver *et al.* (2017) determined averaged lithology specific total stress values for Holocene coastal deposits in the Netherlands: peat 11 kPa, clay 14 kPa, sandy clay 16 kPa, sand 20 kPa, and anthropogenic brought-up soil 18 kPa. These values have been implemented in GeoTOP and were used to quantify total stress at each sampled level. Hydrostatic pressure is 0 kPa at the phreatic groundwater level and increases downward with 10 kPa per metre. The openly available two-dimensional grid of current phreatic groundwater levels in the Netherlands was used (250 $\times$ 250 m) (NHI, 2016) to quantify hydrostatic pressure at each sampled level. Subsequently, the total stress and hydrostatic pressure values were used to calculate vertical effective stress exerted on the sampled intercalated peat layers.

RESULTS

The full intercalated peat dataset, after pairing with a reference level, shows vertical displacements of the peat layers range from –3.1 to 8.1 m (Figure 4). A calculation outcome of positive values (77%) implies that the peat layer has post-depositionally subsided, whereas negative values (23%) indicate a mismatch owing to underestimation of the reference levels. The negative values especially comprise peat beds formed between 6000 and 3000 cal BP, situated in the NW part of the coastal plain (Figure 5). These samples derive from peat

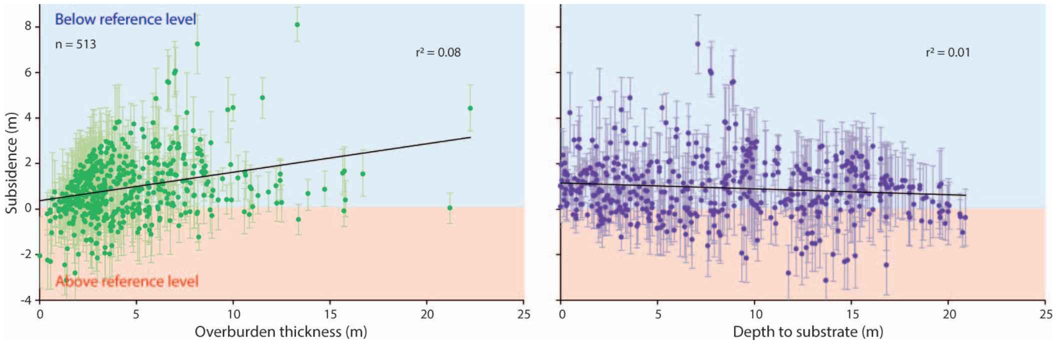

Figure 4. Scatter plots of the amount of subsidence of intercalated peat beds relative to their initial level of formation plotted against present overburden and present depth to substrate that predict peat compression. The vertical error bars represent the GWL uncertainty (σ_{GWL}). (Color for this figure is available in the online version of this paper.)

layers formed fringing tidal inlets and basins (De Mulder and Bosch, 1982) in the part of the study area for which it was known that the 3D GWL interpolation was missing tidal effects (Koster, Stafleu, and Cohen, 2016).

Figure 6 shows a subset of the intercalated peat beds formed between 6350 and 5350 BP (5850 cal BP ± 500 y) and 4000 and 3000 BP (3500 cal BP ± 500 y), projected on palaeogeographic maps of the Netherlands (Vos, 2015). The blue data points represent intercalated peat layers that are situated below their reference level, and those in red represent layers above that level. A pattern emerges, showing that the majority of the samples that are positioned above their reference level are distributed around open tidal basins (left panel) and along silting up tidal inlets (right panel). The mean distances above coeval reference levels are 0.43 ± 0.43 m for the open tidal basin situation and 0.63 ± 0.73 m for the silting up tidal inlet. This vertical distance is lower than the *ca.* 1 m offset between mean sea level and mean high water that prevailed during the last 6000 years (Van der Spek, 1994). Therefore, the shallow buried samples are considered to have experienced postdepositional subsidence of *ca.* 0.5 m. In further analysis, samples deriving from peat layers fringing tidal inlets were discarded based on the palaeogeographic maps of Vos (2015) (Figure 6).

In the fluvial dominated part of the delta, far fewer peat samples are identified as positioned above contemporary reference levels. The few that are might well be from confined floodbasins, where groundwater level can rise locally at times of developing river avulsion (Van Asselen, Cohen, and Stouthamer, 2017).

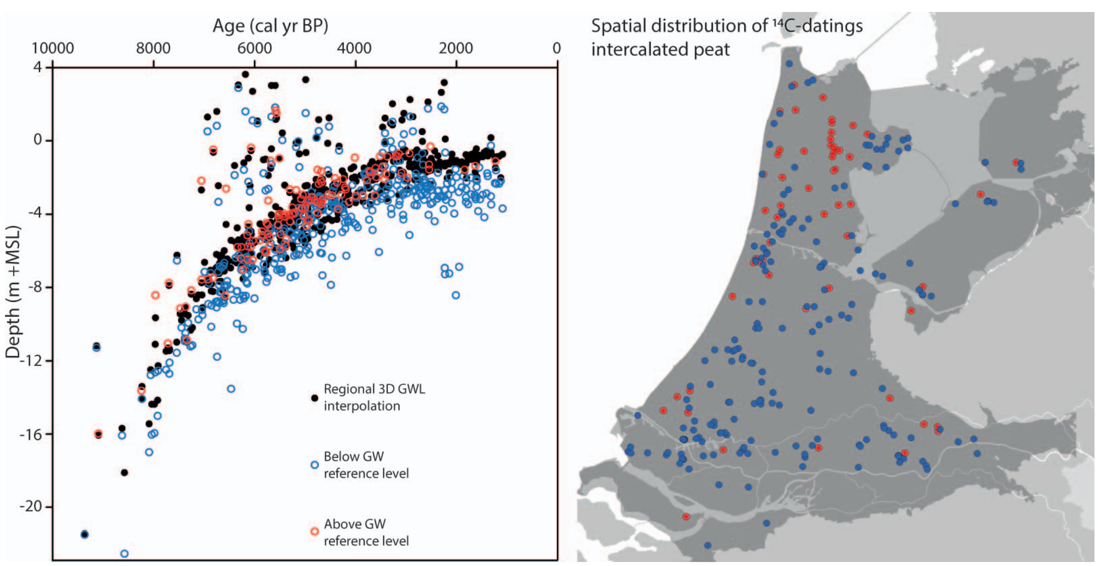

Figure 5. (Left) Black dots represent the elevation of the reference levels for each ^{14}C-dated intercalated peat sample obtained from a 3D GWL interpolation (Koster, Stafleu, and Cohen, 2016). Blue circles are intercalated peat (this study) encountered below the reference level, red circles above. (Right) Spatial distribution of sample depths presently below and above the reference level. The shaded area indicates the lateral extent of the 3D GWL interpolation. (Color for this figure is available in the online version of this paper.)

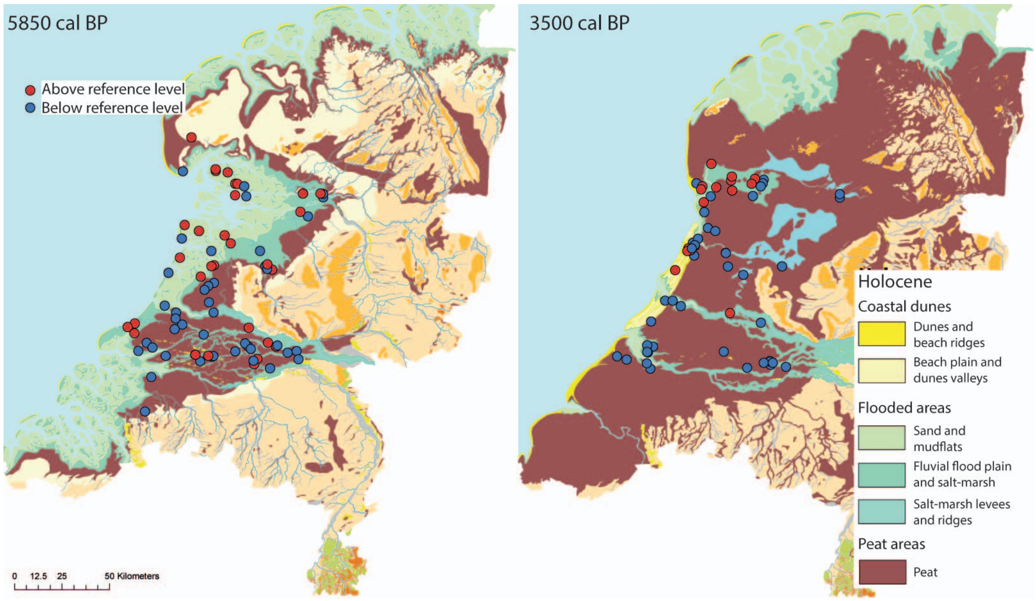

Figure 6. Palaeogeographic maps of 5850 cal BP and 3500 cal BP of the Netherlands (Vos, 2015), with the sampling positions of ^{14}C-dated peat beds formed during these periods (1000 y window centred on these ages). At sampling locations in blue, subsidence below reference level is reproduced. At locations in red—from tidally affected areas mostly—intercalated peat beds plot above supposed contemporary reference level, identifying subsidence underestimation. (Color for this figure is available in the online version of this paper.)

Regression Relations on Constrained Data Subsets

The large scatter resulting from using the vertical-displacement dataset in raw form—with the tidally affected areas and the underestimation of the reference-level heights—also echoes in the linear regression analysis. It yields no correlation with overburden thickness ($r^2 = 0.08$) and depth to substrate ($r^2 = 0.01$) (Figure 4). Standard deviations of the residuals between measured and predicted subsidence are 1.3 m for overburden and 1.4 m for depth to substrate. In view of mapping subsidence, the regression relation was improved by constraining the dataset to only ^{14}C-dating deriving from peat formed between 5000 and 1000 cal BP on top of clastic coastal deposits (seaward side Figure 3). This subset of peat ($N = 127$ ^{14}C-dated peat layers) has vast spatial coverage (*ca.* 5000 km^2; Figure 2B) and occupies relatively shallow positions (Figure 3). A further reason to focus on the shallow back-barrier peat is that its contribution to subsidence is regarded as the highest within the Holocene coastal plain (Erkens, Van der Meulen, and Middelkoop, 2016).

Linear regression analysis on the back-barrier peat subset yielded stronger correlation with overburden thickness ($r^2 = 0.54$; $p = 8E–23$), whereas substantial scatter remained in the regression *vs*. depth to substrate ($r^2 = 0.01$) (Figure 7). In the back-barrier area, subsidence of peat beds relates to overburden thickness (both in metres) as: $subsidence = 0.46 \times overburden + 0.53$.

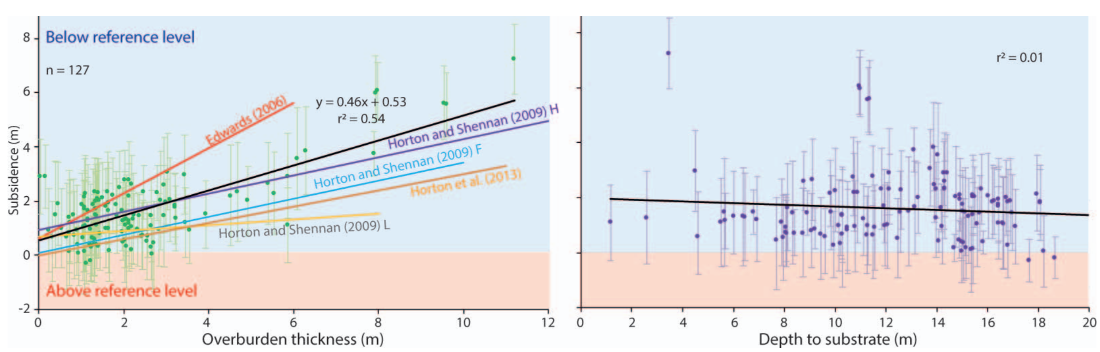

Figure 7. Subsidence scatter plots as in Figure 3, for present overburden and present depth to substrate, but for a subset of peat samples younger than 5000 years. Trend lines of Edwards (2006); Horton and Shennan (2009): H (Humber estuary), F (Fenlands), L (Lincolnshire); Horton *et al*. (2013) are displayed in the left panel. (Color for this figure is available in the online version of this paper.)

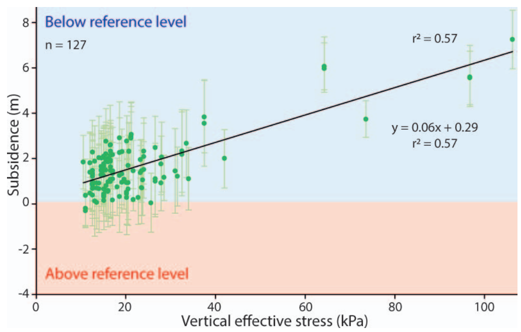

Figure 8. Scatter plot of subsidence of a peat bed within the Holocene sequence *vs*. vertical effective stress exerted on the sampled peat beds, and regression relations describing the subsidence. (Color for this figure is available in the online version of this paper.)

The poor correlation between vertical displacement and depth to substrate indicates that subsidence of the peat beds was not due to compression of the Holocene tidal deposits that underlie the back-barrier peats. In turn, this implies that compression of the back-barrier peat layer itself explains the subsidence. This can be attributed to the composition of these tidal deposits, where sandy and silty clays dominate. Clastic sediments have a relatively low compressibility (*e.g.*, Mesri and Ajlouni, 2007), and therefore the tidal basin sediments will require several metres of overburden to obtain observable compression. That compression behaviour stands in strong contrast to the compressibility of the back-barrier peats. In the peat layers, compression already manifests at decimetres of overburden and lowering of hydrostatic pressure. This is exemplified by Koster, Erkens, and Zwanenburg (2016); they found compression of the Holland coastal plain peat by a 6 m thick earthen embankment reduced *ca*. 90% of its thickness, while it only reduced *ca*. 10% of the thickness of the underlying clayish tidal basin deposits. Since only a few samples of the Holland coastal plain derive from peat with an overburden exceeding 6 m, it is stated that the overburden at the sample locations was insufficient to compress the tidal basin deposits. This is supported by the relatively uniform depth (–4.4 ± 1.2 m mean sea level over *ca*. 5000 km^2) of the bottom of the back-barrier peat layer as modelled in GeoTOP. However, the low compressibility of the tidal basin deposits sustained the relation between peat overburden and subsidence, since compression of the tidal basin deposits would have overprinted the linear relation between overburden and subsidence.

In Figure 8, the relation between the subsidence of the ^{14}C-dated back-barrier peat samples and the vertical effective stress resulting from overburden is shown ($r^2 = 0.57$; $p = 9E–25$). The incorporation of the heterogeneity of overburden shows little improvement of the correlation. According to vertical effective stress–strain diagrams of soft soil compression, strong relations exist between increasing vertical effective stress and thickness reduction of peat (Den Haan, 1994). This small increase of the correlation is explained by the little variation in density that exists within the different types of overburden material; furthermore, the still moderate correlation likely results from the uncertainties in the true depth of the reference levels.

Mapping the Current State of Peat Compression

The linear relation between the thickness of overburden and subsidence of the Holland coastal plain peat (Figure 7, for location see Figure 2B) was deployed to map the subsidence (Figure 9A). The results show that peat layers situated below thick natural and anthropogenic overburden experienced most subsidence by compression. This is particularly the case in the raised centres of the cities of Amsterdam, Rotterdam, and Gouda. Here, shallow peat was first overlain by flood deposits from fluvial and coastal origin, and subsequently by anthropogenic brought-up soil, which is between 1 to 8 m in thickness, and responsible for subsidence ranging from 1 to 5 m. At the inland boundaries of this peat layer the overburden is at most several decimetres thick, and consequently the peat generally has experienced less than 1 m of subsidence. This is also the situation in the agricultural areas north of Amsterdam and near the former Rhine estuary, where peat occurs near the present surface. In the agricultural areas east of Rotterdam, where peat locally is overlain by 1 to 5 m thick fluvial overbank deposits, peat experienced 1 to 3 m of subsidence.

DISCUSSION

This study revealed that reconstructing postdepositional vertical displacements of ^{14}C-dated peat samples relative to reference levels is possible at a regional scale. However, at a regional scale, the method relies heavily on the accuracy of the reference level and on the validity of the linear regression between thickness of overburden and peat compression, which in this case was only true for a specific data subset. The linear regression approach simplifies the processes that caused compression and suffers from considerable uncertainty in the determination of index points. This may become problematic for application at national scale with original data collected in various projects and with different objectives, when compared with its application to a single tidal system where the researcher can more fully control sampling quality. Nevertheless, the results for sites that are at a greater distance from tidal systems show a robust overview of past subsidence. When compared with estimates based on soil-mechanical methods that may suffer from fundamental problems in specifying input parameters for peat behaviour and initial conditions in such heterogeneous areas, the application of ^{14}C-dating as a new method for mapping past peat compression is considered justifiable.

Previously Developed Subsidence Map

A recent reconstruction of peat subsidence in the Holland coastal plain by Erkens, Van der Meulen, and Middelkoop (2016) was established by estimating subsidence from the vertical offset between the current land surface and a reconstructed AD 1000 surface. The contribution of peat compression to this subsidence was quantified using increases in dry organic matter bulk densities relative to pristine uncompressed peat (*cf*. Van Asselen, 2011). Their results show that *ca*. 28% of the subsidence is due to peat compression. In Figure 9B, spatial differences between their reconstructed subsidence by peat compression and the reconstructed subsi-

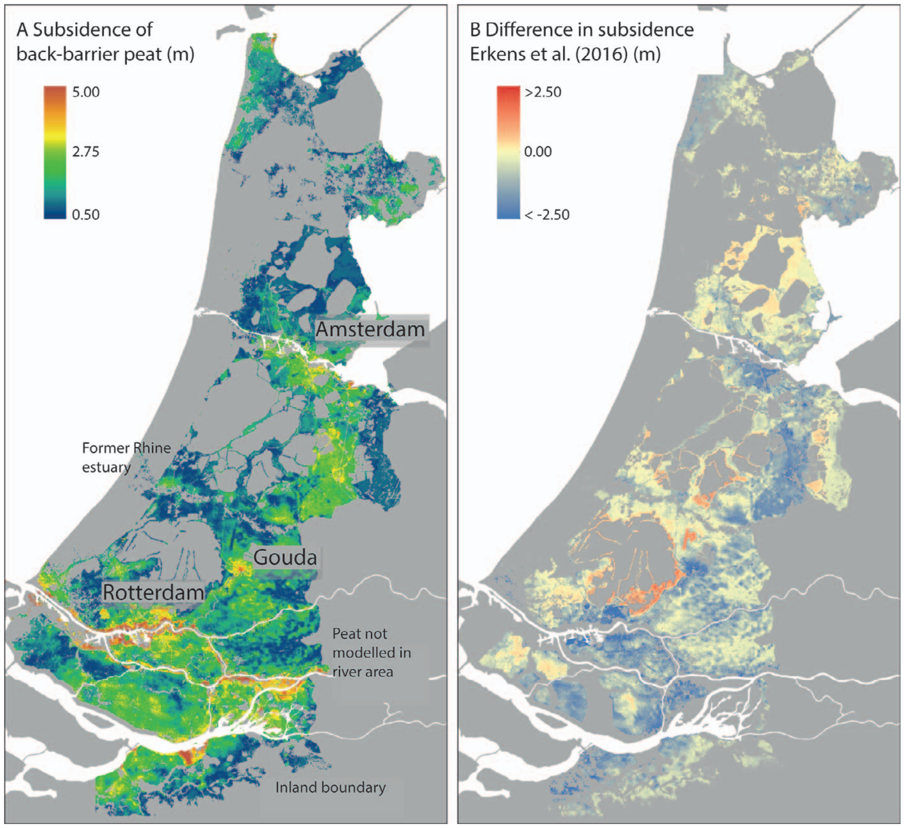

Figure 9. (A) Map depicting subsidence the back-barrier peat experienced by compression (GeoTOP; TNO-GSN, 2016). (B) Map showing the difference in reconstructed subsidence by compression of the back-barrier peat by Erkens, Van der Meulen, and Middelkoop (2016) and this study. (Color for this figure is available in the online version of this paper.)

dence of this study are shown. On average, subsidence by peat compression quantified by Erkens, Van der Meulen, and Middelkoop (2016) is 0.74 m less than subsidence quantified here. This accounts for areas with more than 2 m overburden in particular, such as cities and areas where peat is overlain by overbank deposits. In contrast, their reconstructed subsidence exceeds ours in areas where peat is overlain by less than 2 m overburden, primarily in agricultural areas. These differences primarily arise because Erkens, Van der Meulen, and Middelkoop (2016) assumed less than 1.5 m overburden over the entire area, while this study comprises large areas with more than 1.5 m overburden. Consequently, in areas with less than 2 m overburden, *i.e*. areas with conditions comparable to those in Erkens, Van der Meulen, and Middelkoop (2016), their estimates were within 18 cm of the results presented here.

Reconstructed Peat Compression at Other Coastal-Deltaic Sites

It is widely acknowledged that spatial variation exists in peat compression by overburden, due to spatial differential physical peat properties (Den Haan, 1994; Mesri and Ajlouni, 2007). Variation in physical peat properties is attributable to differences in environmental conditions during and after peat formation. For instance, Den Haan (1994) determined that peat containing sediments and small wood particles is less compressible than highly organic fibrous peat. Furthermore, Den Haan and Kruse (2007) showed that differences exist in time-dependent creep rates, which causes spatial differential reduction in peat compressibility as well. With the reference-level approach, spatial differences in peat compression between different coastal-deltaic sites are also revealed. The presented regression function: $subsidence = 0.46 \times overburden + 0.53$ (Figure 7) has a slope of 0.46, stating that 1 m of overburden causes 0.46 m of vertical displacement by peat compression. In Figure 7, regression functions deriving from other studies focusing on reconstructing peat compression with ^{14}C-dating are shown. The slopes of functions developed for several sites at the coastal zone of the U.K. have an average of 0.40 (Edwards, 2006; Horton and Shennan, 2009 [with a positive intercept only]). A maximum slope of 0.84 was obtained by Edwards (2006) (Loughor Estuary), whereas a minimum of 0.11 was found by Horton and Shennan (2009) (Lincolnshire). Horton *et al*. (2013) obtained a slope 0.30 for a site at the coast of New Jersey, United States. This emphasizes the need for local to regional calibration of the regression function, when applying this method in other areas.

Furthermore, the regression function has an intercept of 0.53, indicating that 0.53 m of subsidence occurred regardless of overburden. Intercepts of multiple decimetres were also obtained by Edwards (2006) (0.6 m) and Horton and Shennan (2009) (site Lincolnshire 0.7 m; site Humber estuary 0.9 m). According to Törnqvist *et al*. (2008), this positive intercept is due to compression of underlying Holocene deposits. However, for the Netherlands this could also be due to the reduction of hydrostatic pressure by groundwater level lowering during reclamation or time-dependent creep processes prevailing since the onset of peat formation. Koster, Erkens, and Zwanenburg (2016) determined by using widely acknowledged soil-mechanic concepts that creep reduced the thickness of peat embedded in the Holland coastal plain by *ca*. 20% in 4000 years, that is, between onset of peat formation and the reclamation of the wetlands.

The map presented in this study indicates that subsidence by compression of the back-barrier peat during the past 1000 years primarily ranges between *ca*. 0.5 to 5 m. This is caused by overburden with a spatially varying thickness between *ca*. 0 and 10 m. Törnqvist *et al*. (2008) quantified *ca*. 1 to 5 m subsidence by compression of a peat layer over a *ca*. 5 km long profile in the Mississippi delta. The overburden consisted of *ca*. 2 to 11 m of natural levee deposits that began to form *ca*. 1500 years ago. Long, Waller, and Stupples (2006) determined *ca*. 3 m of peat compression due to the presence of 4.8 m of overburden consisting of tidal deposits in Romney Marsh (U.K.). These tidal deposits caused subsidence of the peat from *ca*. 1200 years ago onward. This indicates that the presented subsidence map is in good agreement with these previously made observations in other settings.

CONCLUSIONS

This paper presents an approach to map regional scale vertical displacement of Holocene peat layers below their reference groundwater levels in the Holland coastal plain of the Netherlands using quantifications of subsidence induced by compression of ^{14}C-dated peat layers. The quantification was conducted by determining the vertical interval between the current and initial level of intercalated peat layers. The initial level was determined using a 3D interpolation of Holocene GWL for the entire coastal area. With regression analysis, the amount of peat compression was related to overburden. By implementing this relation in the 3D GeoTOP geological model, a map was obtained showing the subsidence a back-barrier peat layer experienced by compression.

The urbanized areas in the coastal plain experienced 1 to 5 m of peat compression in response to loading by flood deposits and anthropogenic brought-up soil. In the agricultural areas, peat compression generally resulted in less than 1 m of subsidence, with local maxima of 3 m. Maxima values were obtained in particular in areas overlain by deposits from river flooding and sea ingressions. In agricultural areas without overburden, subsidence has been *ca*. 0.5 m owing to reducing hydrostatic pressure during peat reclamation.

Gaining a better insight and understanding at the regional scale of the amounts and spatial variation of past subsidence due to peat compression is essential to managing present and future subsidence. This relates to differences in (1) land use, *i.e*. urbanized areas *vs*. agricultural lands, and (2) past coastal and fluvial dynamics, specifically flooded areas with natural overburden covering the peat *vs*. areas with peat at the present surface.

ACKNOWLEDGMENTS

This work is part of the PhD research of KK, financed and facilitated by TNO-GSN. Hans Middelkoop is thanked for supervision and critically reading the manuscript during an earlier stage, Freek Busschers is acknowledged for his suggestions, and Gilles Erkens is thanked for sharing his subsidence grid of the Holland coastal plain peat. We are indebted to Nikki Trabucho for graphically improving Figure 3. This paper greatly benefited from the comments of three anonymous reviewers.

LITERATURE CITED

Bloom, A.L., 1964. Peat accumulation and compaction in a Connecticut coastal marsh. *Journal of Sedimentary Research*, 3(3), 599–603.

Borger, G.J., 1992. Draining-digging-dredging; the creation of a new landscape in the pat areas of the low countries. *In:* Verhoeven, J.T.A. (ed.), *Fens and Bogs in the Netherlands: Vegetation, History, Nutrient Dynamics and Conservation. Geobotany*, *Volume 18*. Dordrecht, the Netherlands: Springer, pp. 237–322.

Bos, I.J.; Busschers, F.S., and Hoek, W.Z., 2012. Organic-facies determination: A key for understanding facies distribution in the basal peat layer of the Holocene Rhine-Meuse delta, the Netherlands. *Sedimentology*, 59(2), 676–703. doi: 10.1111/j.1365-3091.2011.01271.x

Brain, M.J., 2016. Past, present and future perspectives of sediment compaction as a driver of relative sea level and coastal change. *Current Climate Change Reports*, 2, 75–85. doi: 10.1007/s40641-016-0038-6

Brain, M.J.; Long, A.J.; Woodroffe, S.A.; Petley, D.N.; Milledge, D.G., and Parnell, A.C., 2012. Modelling the effects of sediment compaction on salt marsh reconstructions of recent sea-level rise. *Earth and Planetary Science Letters*, 345–348, 180–193. doi: 10.1016/j.epsl.2012.06.045

Bronk Ramsey, C., 2009. Dealing with outliers and offsets in Radiocarbon dating. *Radiocarbon*, 51(3), 1023–1045.

Cohen, K.M., 2005. 3D geostatistical interpolation and geological interpretation of paleo groundwater rise in the Holocene coastal prism in the Netherlands. *In:* Giosan, L. and Bhattacharya, J.P. (eds.), *River Deltas—Concepts, Models, and Examples*. *SEPM Special Publication*, Special Issue No. 83, pp. 341–364.

De Mulder, E.F.J. and Bosch, J.H.A., 1982. Holocene stratigraphy, radiocarbon datings and paleogeography of Central and Northern North-Holland (the Netherlands). *Mededelingen van de Rijks Geologische Dienst*, 36, 111–160.

Den Haan, E.J., 1994. Vertical Compression of Soils. Delft, the Netherlands: TU Delft, Ph.D. dissertation, 96p.

Den Haan, E. and Kruse, G.A.M., 2007. Characterisation and engineering properties of Dutch peats. *Characterisation and Engineering Properties of Natural Soils* 3, 2101–2133, doi:10.1201/NOE0415426916.ch13

Den Held, A.J.; Schmitz, M., and Van Wirdum, G., 1992. Draining-digging-dredging; the creation of a new landscape in the peat areas of the low countries. *In:* Verhoeven, J.T.A. (ed.), *Fens and Bogs in The Netherlands: Vegetation, History, Nutrient Dynamics and Conservation. Geobotany*, *Volume 18*. Dordrecht, the Netherlands:-Springer, pp. 237–322.

Drexler, J.Z.; De Fontain, C.S., and Deverel, S.J., 2009. The legacy of wetland drainage on the remaining peat in the Sacramento—San Joaquin Delta, California, USA. *Wetlands*, 29(1), 372–386.

Edwards, R.J., 2006. Mid- to late-Holocene relative sea-level change in southwest Britain and the influence of sediment compaction. *The Holocene*, 16(4), 575–587. doi: 10.1191/0959683606hl941rp

Erkens, G.; Van der Meulen, M., and Middelkoop, H., 2016. Double trouble: Subsidence and CO_2 respiration due to 1000 years of cultivation of the Dutch coastal peatlands. *Hydrogeology Journal*, 24, 551–568. doi: 10.1007/s10040-016-1380-4

Gambolati, G.; Putti, M.; Teatini, P., and Gasparetto Stori, G., 2006. Subsidence due to peat oxidation and impact on drainage infrastructures in a farmland catchment south of the Venice Lagoon. *Environmental Geology*, 46(6), 814–820. doi: 10.1007/s00254-006-0176-6

Higgins, S.A., 2016. Advances in delta-subsidence research using satellite methods. *Hydrogeology Journal*, 24, 587–600. doi: 10.1007/s10040-015-1330-6

Hooijer, A.; Page, S.; Jauhiainen, W.; Lee, W.A.; Lu, X.X.; Indris, A., and Anshari, G., 2012. Subsidence and carbon loss in drained tropical peatlands. *Biogeosciences*, 9, 1053–1071. doi: 10.5194/bg-9-1053-2012

Horton, B.P.; Engelhart, S.E.; Hill, D.F.; Kemp, A.C.; Nikita, D.L.; Miller, K.G., and Peltier, W.R., 2013. Influence of tidal-range change and sediment compaction on Holocene relative sea-level change in New Jersey, USA. *Journal of Quaternary Science*, 24, 403–411. doi: 10.1002/jqs.2634

Horton, B.P. and Shennan, I., 2009. Compaction of Holocene strata and the implications or relative sea-level change on the east coast of England. *Geology*, 37(12), 1083–1086. doi: 10.1130/G30042A.1

Huizinga, T.K., 1940. De bodemdaling van Nederland bezien van een grondmechanisch standpunt (in Dutch). *Geologie en Mijnbouw*, 2, 259–277.

Kiden, P.; Denys, L., and Johnston, P., 2002. Late Quaternary sea-level change and isostatic and tectonic land movements along the Belgian-Dutch North Sea coast: Geological data and model results. *Journal of Quaternary Science*, 17, 535–546. doi: 10.1002/jqs.709

Kluiving, S.; De Ridder, T.; Van Dasselaar, M.; Roozen, S., and Prins, M., 2016, Soil archives of a Fluvisol: Subsurface analysis and soil history of the medieval city centre of Vlaardingen, the Netherlands—An integral approach. *Soil*, 2, 271–285.

Kooi, H.; Johnston., P.; Lambeck, K.; Smither, C., and Molendijk, R., 1998. Geological causes of recent (~100 yr) vertical land movement in the Netherlands. *Tectonophysics*, 299, 297–316.

Koster, K., 2016. Cone Penetration Testing: A sound method for urban archaeological prospection. *Archaeological Prospection*, 23(1), 55–69. doi: 10.1002/arp.1531

Koster, K.; Erkens, G., and Zwanenburg, C., 2016. A new soil mechanics approach to quantify and predict land subsidence by peat compression. *Geophysical Research Letters*, 43(20), 10792–10799. doi: 10.1002/2016GL071116

Koster. K.; Stafleu, J., and Cohen, K.M., 2016. Generic 3D interpolation of Holocene base-level rise and provision of accommodation space, developed for the Netherlands coastal plain and infilled palaeovalleys. *Basin Research*, 29(6), 775–797. doi: 10.1111/bre.12202

Kruiver, P.; Van Dedem, E.; Romin, R.; De Lange, G.; Korff, M.; Stafleu, J.; Gunnink, J.L.; Rodriguez-Marek, A.; Bommer, J.J.; Van Elk, J., and Doornhof, D., 2017. An integrated shear-wave velocity model for the Groningen gas field, the Netherlands. *Bulletin of Earthquake Engineering*, 9, 3555–3580. doi: 10.1007/s10518-017-0105-y

Long, A.J.; Waller, M.P., and Stupples, P., 2006. Driving mechanisms of coastal change: Peat compaction and the destruction of late Holocene coastal wetlands. *Marine Geology*, 225(1–4), 63–84. doi: 10.1016/j.margeo.2005.09.004

Massey, A.C.; Paul, M.A.; Gehrels, W.R., and Charman, D.J., 2006. Autocompaction in Holocene coastal back-barrier sediments from south Devon, southwest England, UK. *Marine Geology*, 226, 225–241. doi: 10.1016/j.margeo.2005.11.003

Mazzotti, S.; Lambert, A.; Van der Kooij, M., and Mainville, A., 2009. Impact of anthropogenic subsidence on relative sea-level rise in the Fraser River delta. *Geology*, 37, 771–774. doi: 10.1130/G25640A.1

Meckel, T.A.; Ten Brink, U.S., and Williams, S.J., 2007. Sediment compaction rates and subsidence in deltaic plains: Numerical constraints and stratigraphic influences. *Basin Research*, 19, 19–31. doi: 10.1111/j.1365-2117.2006.00310.x

Mesri, G. and Ajlouni, M., 2007. Engineering properties of fibrous peats. *Journal of Geotechnical and Geoenvironmental Engineering*, 133, 850–866. doi: 10.1016/(ASCE)1090-0241(2007)133:7(850).

NHI (Nederlands Hydrologisch Instrumentarium), 2016. *Hydrological data of the Netherlands*. www.nhi.nu.

Pierik, H.J.; Cohen, K.M.; Vos, P.C.; Van der Spek, A.J.F., and Stouthamer, E., 2017. Late Holocene coastal-plain evolution of the Netherlands: The role of natural preconditions in human-induced sea ingressions. *Proceedings of the Geologists' Association*, 128(2), 180–197. doi: 10.1016/j.pgeola.2016.12.002

Reimer, P.J.; Bard, E.; Bayliss, A.; Beck, J.W.; Blackwell, P.G.; Bronk Ramsey, C.; Buck, C.E.; Cheng, H.; Edwards, R.L.; Friedrich, M.; Grootes, P.M.; Guilderson, T.P.; Haflidason, H.; Hajdas, I.; Hatté, C.; Heaton, T.J.; Hoffmann, D.L.; Hogg, A.G.; Hughen, K.A.; Kaiser, K.F.; Kromer, B.; Manning, S.W.; Niu, M.; Reimer, R.W.; Richards, D.A.; Scott, E.M.; Southon, J.R.; Staff, R.A.; Turney, C.S.M., and Plicht, J.V.D., 2013. IntCal13 and Marine13 radiocarbon age calibration curves 0–50,000 years cal BP. *Radiocarbon*, 55, 1869–1887. doi: 10.2458/azu_js_rc.55.16947

Roberts, H.H.; Bailey, A., and Kuecher, G.J., 1994. Subsidence in the Mississippi River Delta—Important influences of valley filling by cyclic deposition, primary consolidation phenomena, and early diagenesis. *Gulf Coast Association of Geological Societies Transactions*, 44, 619–629.

Schothorst, C.J., 1977. Subsidence of low moor peat soils in the western Netherlands. *Geoderma*, 17, 265–291.

Shennan, I.; Lambeck, K.; Horton, B.P.; Innes, J.; Lloyd, J.; McArthur, J., and Rutherford, M., 2000. Holocene isostasy and relative sea-level changes on the east coast of England. *In:* Shennan, I. and Andrews, J. (eds.), *Holocene Land-Ocean Interaction and Environmental Change around the North Sea*. *Geological Society, London*. Special Issue No. 166, pp. 275–298

Stafleu, J.; Maljers, D.; Gunnink, J.L.; Menkovic, A., and Busschers, F.S., 2011. 3D modelling of the shallow subsurface of Zeeland, the Netherlands. *Netherlands Journal of Geosciences*, 90(4), 293–310. doi: 10.1017/S0016774600000597

Stouthamer, E. and Van Asselen, S., 2015. Potential of Holocene deltaic sequences for subsidence due to peat compaction. *Proceedings of the IAHS*, 372, 173–178. doi: 10.5194/piahs-372-173-2015

Syvitski, J.P.M.; Kettner, A.J.; Overeem, I.; Hutton, E.W.H.; Hannon, M.T.; Brakenridge, G.R.; Day, J.; Vörösmarty, C.; Saito, Y.; Giosan, L., and Nicholls, R.J., 2009. Sinking deltas due to human activities. *Nature Geoscience*, 2, 681–686. doi: 10.1038/ngeo629

TNO-GSN (Netherlands Organisation for Applied Scientific Research—Geological Survey of the Netherlands), 2016. *Digital geoproducts Geological Survey of the Netherlands*. www.dinoloket.nl/en.

Törnqvist, T.E.; Wallace, D.J.; Storms, J.E.A.; Wallinga, J.; Van Dam, R.L.; Blaauw, M.; Derksen, M.S.; Klerks, C.J.W.; Meijneken, C., and Snijders, E.M.A., 2008. Mississippi Delta subsidence primarily caused by compaction of Holocene strata. *Nature Geoscience*, 1, 173–176. doi: 10.1038/ngeo129

Van Asselen, S., 2011. The contribution of peat compaction to total basin subsidence: Implications for the provision of accommodation space in organic-rich deltas. *Basin Research*, 23(2), 239–255. doi: 10.1111/j.1365-2117.2010.00482.x

Van Asselen, S.; Cohen, K.M., and Stouthamer, E., 2017. The impact of avulsion on groundwater level and peat formation in delta floodbasins during the Middle Holocene transgression in the Rhine-Meuse delta, the Netherlands. *The Holocene*, 27(11), 1694–1706. doi: 10.1177/0959683617702224

Van Asselen, S.; Stouthamer, E., and Van Asch, Th.W.J., 2009. Effects of peat compaction on delta evolution: A review on processes, responses, measuring and modelling. *Earth Sciences Reviews*, 92, 35–52. doi: 10.1016/j.earscirev.2008.11.001

Van de Plassche, O., 1995. Periodic clay deposition in a fringing peat swamp in the lower Rhine-Meuse river area, 5,400–3,400 cal BC. *In:* Finkl, C.W. (ed.), *Holocene Cycles: Climate, Sea Levels, and Sedimentation. Journal of Coastal Research*, Special Issue No. 17, pp. 95–102.

Van den Born, G.J.; Kragt, F.; Henkens, D.; Rijken, B.; Van Bemmel, B., and Van der Sluis, S., 2016. *Dalende bodem, stijgende kosten* (in Dutch). Planbureau voor de Leefomgeving, The Hague, the Netherlands, pp. 94.

Van der Spek, A.J.F., 1994. Large-Scale Evolution of Holocene Tidal Basins in the Netherlands. Utrecht, the Netherlands: Utrecht University, Ph.D. dissertation, 191p.

Vis, G.J.; Westerhoff, W.E.; Ten Veen, J.H.; Hijma, M.P.; Van der Spek, A.J.; Vos, P.C., and Cohen, K.M., 2015. Chapter 33: Paleogeography. *In:* Shennan, I.; Long, A.J., and Horton, P.H. (eds.), *Handbook of Sea-Level Research*. Hoboken, New Jersey: Wiley-Blackwell, American Geophysical Union, pp. 600.

Vos, P.C., 2015. Origin of the Dutch Coastal Landscape. Utrecht, The Netherlands: Utrecht University, Ph.D. dissertation, 358p.

Wösten, J.H.M.; Ismail, A.B., and Van Wijk, A.L.M., 1997. Peat subsidence and its practical implications: A case study in Malaysia. *Geoderma*, 78, 25–36.